Stress/Displacement Field Calculation for Discontinuous Mechanical Structure Based on Layered Elastic Theory

†Qingchao Sun, *Liangguo Meng, Yunlong Wang and Lin Xue

School of Mechanical Engineering, Dalian University of Technology, China

*Presenting author: menglg@mail.dlut.edu.cn
†Corresponding author: qingchao@dlut.edu.cn

Abstract

Stress/displacement field analyzing of mechanical assembly is the basis of predicting the mechanical property of the assembly and optimizing the structure and the assembly process. However, the discontinuity structures in the mechanical make it difficult to calculate. In this paper, a new kind of stress/displacement layered mapping and calculation method based on layered elastic theory is proposed. With considering the mechanical continuous/discontinuous characteristics, a layered model of assembly structure is established and the layered constraint conditions is determined by its position in assembly. Stress/displacement field could be obtained by using traditional solution of layered elastic system which is modified to adjust to the model of mechanical assembly. Finally, a discontinuous mechanical structure is solved by using the layered model and the comparison between the analytically calculation, FEA and experiment data proves the effectiveness of the model.

Keywords: Stress/displacement field; Layered elastic theory; Structural discontinuity; Elastic mechanics

1 Introduction

In general, machines like lathe are not a continuous whole. They're assembly by various parts according to requirements. The parts that are connected to each other are called mechanical joints, such as bolted joint, sliding guide joint, et al. The contact region between different parts of the ministry is often referred to as a joint interface.

According to the research, the characteristics of mechanical joint interface have an important influence on the performance of mechanical parts, such as contact fatigue strength, friction power consumption, wear life [1,2,3]. In addition, the dynamic performance, vibration and noise of mechanical equipment depend on interface's stiffness and the damping. Burdekin et al [4] pointed out that the deformation of machine tool's joints accounted for most of the total deformation and the contact stiffness of joints was about 60%~80% of the total rigidity of the machine tool. The research of Yagi[5] found that the mechanical joint is important to the dynamic stiffness of reconfigurable machine tool. There is a view [6] joint's damping is larger than the damping of the structure itself and Beards [7,8,9] studied structure damping with the interface's sliding. He puts the integration that 90% of the total damping is coming from joint. Now that the joint is significant on the static and dynamic performance of mechanical system, a lot of researches have been carried out. For instance, Zhang and Mr. Huang [10, 11] had studied joint's normal and tangential stiffness, damping through a lot of experiments and summarized the influence of normal stress, the media, materials, processing methods and roughness. Mi [12] studied the influence of the pretension on the dynamic stiffness of the machine tool. In addition, a lot of achievements have been made in the identification of the parameters and the mechanics modeling of the joint [1,13-15].

In fact, joint's behavior is important for mechanical design/operation/maintenance of mechanical equipment. People has accumulated experiences to analyze it in long-term engineering practice. With the development of science and technology, the joint interface's charactícts of mechanical equipment will become an important part of scientific and technical.

Joint is a space with a certain thickness. In order to understand joint comprehensively and accurately, it is necessary to figure out how the load transforming in joint interface. Traditional mechanical analysis methods, either material mechanics or elastic mechanics, are based on the theory of continuum mechanics and the assumption that the object is composed of a continuous medium filled in the space [16]. The joint in mechanical equipment destroys the continuity of the whole machine structure, so that the continuum mechanics is not completely suitable for the analysis of the assembly mechanical. Moreover, the discontinuity of the structure makes the transfer of load between the components more complex, including non-linearity, which making it difficult to analyze the stress/displacement field in machine.

Layered elastic theory (LET) is the theoretical foundation in pavement design and calculation. LET belong to the elasticity. It developed on the basis of elastic semi-space theory. In 1885, Bossiness proposed a theoretical solution to the stress/displacement of elastic semi-space under vertical concentrated force. In 1943 and 1945, the Burmister used the Love functions to obtain the theoretical solution of the stress/displacement of the double-layer and multi-layer elastic system under the symmetrical vertical load [17-19]. In 1951, Sneddon firstly introduced the Hankel integral transforms into axisymmetric problems [20]. Since then, the LET has been developed rapidly and extended to non-axisymmetric and multi-layer elastic systems [21-24]. With the improvement of computer and computing method, the system of layered elastic mechanics is applied to the engineering. There are lots of algorithms for computing, such as BISAR, JULEA, DIPLOMAT, Kenlayer, LEAF, et al [24]. At present, the layered elastic system mechanics and its algorithm have been widely used in the engineering practice of multi-level road and multi-layer foundation all over the world.

LET is widespread in road construction, but it is seldom used in mechanical. The theory comprehensively considers both overall stress transfer and the discontinuous effect of interface to analyze the stress/ displacement field, which provides the possibility for the analysis of mechanical characteristics of discontinuous mechanical structures.

Therefore, this paper introduces a new method which is based on layered elastic mechanics to analysis stress/ displacement field in discontinuous mechanics. An example of double-layer discontinuous mechanical under vertical load is given and in order to verify the effectiveness, we also have experimental and finite element analysis. Comparing the results of three methods, the new method is effective in structural discontinuity.

2 The Basic Concept of Layered Elastic Theory

The LET is the theoretical basis of multi-layer pavement and foundation design. The pavement system is layered structure on the soil foundation and composed of different materials. In general, the external load on the road surfaces is vertical or horizontal. LET assumes object as an elastic system, including a series of elastic layers and a semi-infinite layer. It is used to analyze stress and displacement of the elastic system when load is acting on the surface of pavement. LET is based on the following assumptions:

- Each layer is ideal linear elasticity, completely uniform, continuous, and isotropic.
- Initial stress is 0 and body forces are ignored in system without external load.
- Strains and displacement are assumed to be small.
- Stress, deformation and displacement vanish in infinity point.

Fig. 1 shows a n-layer elastic system. We denote the number of layers as n. E_i、 μ_i、 h_i are Young's modulus, Poisson's ratio and thickness of layers respectively. Each layer is infinite along radial direction r. Except the n$_{th}$-layer is a semi-infinite space ($h_n = \infty$), the other layers' thickness is limited. The cylindrical coordinate system is established in Fig. 1 and there is only vertical load acting on the surface.

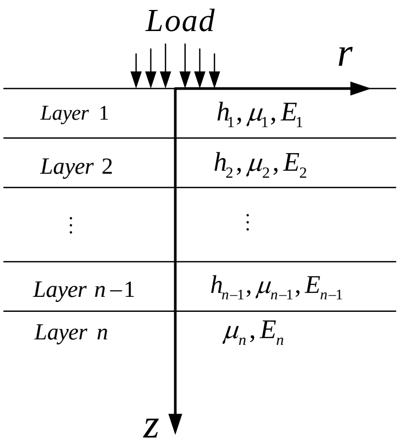

Fig. 1. A n-layer elastic system

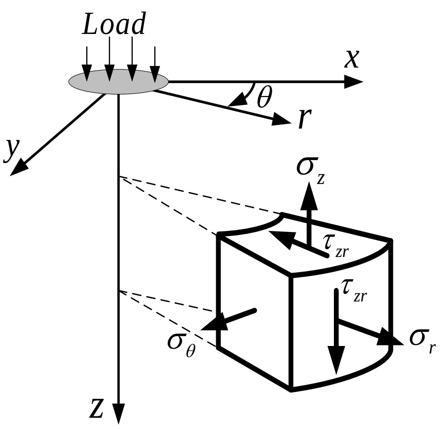

Fig. 2. axisymmetric problem.

There are two main methods based on LET to obtain stress/displacement filed in layered elastic system[23]. The traditional method gives the relation between mechanical component and correlation function firstly. Then the undetermined function is obtained through the Hankel transformation. For example, Burmister presents a unique stress function, which solves the stress and displacement of the two-layer and three-layer elastic system under the axisymmetric vertical load[17]−[19]. Maina and Matsui used the Michell equation and Boussinesq equation to calculate the elastic response of the elastic layered structure under horizontal and vertical loads[22]. It should be pointed out the method is simple and practical, but we must know the relation of displacement/stress component and the displacement/stress function. It is suitable for simple problems such as spatial axisymmetric.

The other method[23] calculates basic equation with the Laplace and Hankel integral transformation to obtain stress/displacement field. Although it does not need to obtain the relation between the displacement/stress component and the displacement/stress function, the process of solution is quite complicated.

The first method (displacement method) is used to solve spatial axisymmetric problem in the next. It is typical method to establish mechanical model in layered elastic system.

The whole solution begins with acquiring stress/displacement's general result in axisymmetric spatial. In cylindrical coordinates system, assuming Love displacement function $\phi(r,z)$ and according to Lame equation of elasticity, the relation between displacement components and displacement function is expressed as follows:

$$\left.\begin{aligned} u &= -\frac{1+\mu}{E}\frac{\partial^2\phi}{\partial r\partial z} \\ w &= \frac{1+\mu}{E}[2(1-\mu)\nabla^2\phi - \frac{\partial^2\phi}{\partial z^2}] \end{aligned}\right\} \tag{1}$$

The stress component is shown by the displacement function

$$\left.\begin{aligned} \sigma_r &= \frac{\partial}{\partial z}(\mu\nabla^2\phi - \frac{\partial^2\phi}{\partial r^2}) \\ \sigma_\theta &= \frac{\partial}{\partial z}(\mu\nabla^2\phi - \frac{1}{r}\frac{\partial\phi}{\partial r}) \\ \sigma_z &= \frac{\partial}{\partial z}[(2-\mu)\nabla^2\phi - \frac{\partial^2\phi}{\partial z^2}] \\ \tau_{zr} &= \frac{\partial}{\partial r}[(1-\mu)\nabla^2\phi - \frac{\partial^2\phi}{\partial z^2}] \end{aligned}\right\} \tag{2}$$

Where ∇^2 denote the Laplace operator and is given by

$$\nabla^2 = \frac{\partial^2}{\partial r^2} + \frac{1}{r}\frac{\partial}{\partial r} + \frac{\partial^2}{\partial z^2} \tag{3}$$

In fact, the Love displacement function should satisfy the following re-harmonic equation

$$\nabla^4\phi = 0 \tag{4}$$

Using the Hankel integral transformation on both ends of the re-harmonic Eq. (3) it can be shown that

$$\int_0^\infty r\nabla^4\phi(r,z)J_0(\xi r)dr = (\frac{d^2}{dz^2} - \xi^2)^2\bar{\phi}(\xi,z) = 0 \tag{5}$$

Where $\bar{\phi}(\xi,z)$ is the zero-order Hankel integral transformation function

$$\bar{\phi}(\xi,z) = \int_0^\infty r\phi(r,z)J_0(\xi r)dr \tag{6}$$

Eq. (4) is the ordinary differential equation, and the expression of its solution is

$$\bar{\phi}(\xi,z) = (C_\xi + A_\xi z)e^{\xi z} + (D_\xi + B_\xi z)e^{-\xi z} \tag{7}$$

The solution of displacement function $\phi(r,z)$ is obtained by the means of Hankel inverse transform

$$\phi(r,z) = \int_0^\infty \xi[(C_\xi + A_\xi z)e^{\xi z} + (D_\xi + B_\xi z)e^{-\xi z}]J_0(\xi r)d\xi \tag{8}$$

Where ξ is integral variable and A_ξ 、 B_ξ 、 C_ξ 、 D_ξ are integral constant associated with ξ.

Assuming $A = \xi^3 A$ ， $B = \xi^2 B$, $C = \xi^3 C$, $D = \xi^2 D$ and substituting Eq. (6) into Eq. (1) and (2), component of stress and displacement are obtained

$$\left.\begin{aligned}
\sigma_r &= \int_0^\infty \xi J_0(\xi r)\left\{\left[C+(1+2\mu+\xi z)A\right]e^{\xi z}-\left[D-(1+2\mu-\xi z)B\right]e^{-\xi z}\right\}d\xi-\frac{1}{r}U \\
\sigma_\theta &= 2\mu\int_0^\infty \xi J_0(\xi r)(Ae^{\xi z}+Be^{-\xi z})d\xi+\frac{1}{r}U \\
\sigma_z &= -\int_0^\infty \xi J_0(\xi r)\left\{\left[C-(1-2\mu-\xi z)A\right]e^{\xi z}-\left[D+(1-2\mu_i+\xi z)B\right]e^{-\xi z}\right\}d\xi \\
\tau_{zr} &= -\int_0^\infty \xi J_1(\xi r)\left\{\left[C+(2\mu+\xi z)A\right]e^{\xi z}+\left[D-(2\mu-\xi z)B\right]e^{-\xi z}\right\}d\xi \\
u &= \frac{1+\mu}{E}\int_0^\infty J_1(\xi r)\left\{\left[C+(1+\xi z)A\right]e^{\xi z}-\left[D-(1-\xi z)B\right]e^{-\xi z}\right\}d\xi \\
w &= -\frac{1+\mu}{E}\int_0^\infty J_0(\xi r)\left\{\left[C-(2-4\mu-\xi z)A\right]e^{\xi z}+\left[D+(2-4\mu+\xi z)B\right]e^{-\xi z}\right\}d\xi
\end{aligned}\right\} \tag{9}$$

Where

$$U=\int_0^\infty J_1(\xi r)\left\{\left[C+(1+\xi z)A\right]e^{\xi z}-\left[D-(1-\xi z)B\right]e^{-\xi z}\right\}d\xi \tag{10}$$

Where J_0, J_1 are order 0 and order 1 of the first kind Bessel functions; denoting ξ as integral constant. A_ξ 、 B_ξ 、 C_ξ 、 D_ξ are integral constants associated with ξ and solved through definite condition of question.

If the load is axisymmetric, the mechanical problem in the layered elastic system also belongs to spatial axisymmetric problems. Since Eq. (9) is a general solution of stress/displacement in spatial axisymmetric problems, the stress displacement at any point in the layered elastic system can be solved. The stress and displacement expressions in Eq. (9) contain four integral constants A 、 B 、 C 、 D . As long as the integral constant is determined, the stress/displacement of the entire layered elastic system can be obtained. Because the boundary conditions of each layer are different, the integral constants in the stress/displacement expression of each layer are also different. In this paper, the subscript i is used to number the layers. In a N-layer elastic system, there are 4N unknown integral constants, A_i , B_i , C_i , $D_i\ (i=1,2,\ldots,N)$.

It is known when the surface of layers contacts or bond, the normal stress (displacement) on both sides of interface is continuous and the tangential stress (displacement) may have some correlation. Furthermore, it is easy to obtain the stress boundary conditions in the surface of the layered elastic system. By using these stress conditions of surface, bonding conditions between layers and other definite conditions, equation set can be established to solve integral constants. The above is a common method for solving layered elastic mechanics system.

3 Calculation of Discontinuous Mechanical Structure.

3.1 Model Assumption

Different from roadbed structure, the structure of mechanical equipment is more complicated in general. It is necessary to ignore some unimportant factors and simplify the practical problems. In this paper, the discontinuous mechanical structure with vertical load is simplified as the following model, a double-layer elastic system. The system bases on the assumption of LET.

In Fig. 3, we denote the thickness of layer 1 as h and the layer 2 is a semi-infinite substrate. E_i、 μ_i are layers' Young's modulus and Poisson's ratio respectively. The uniform load $q(r)$ is distributed vertically on a circular area (radius δ) on the 1st layer's surface. Because the distribution of load is axisymmetric, the stress, strain and displacement components are also axissymmetry. Stress and displacement of any point in the system could be solved through the traditional method, Love displacement function method. The stress of the axisymmetric problem is shown in.

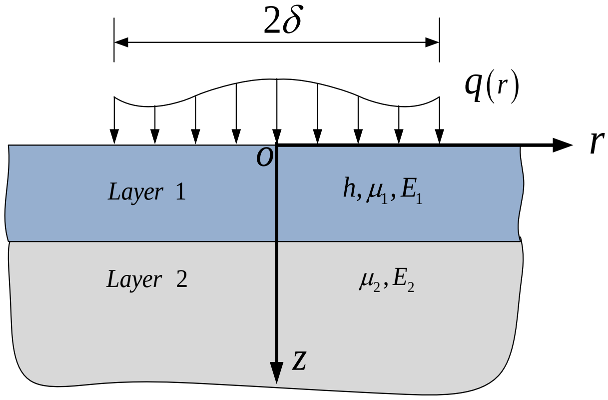

Fig. 3. A double-layer elastic system

3.2 Boundary Conditions and Governing Equations

Since the system is subjected to vertical downward normal force, its surface stress boundary condition is as follows

$$\left.\begin{array}{ll}\sigma_{z1} = -q(r) & (z=0) \\ \tau_{zr1} = 0 & (z=0)\end{array}\right\} \tag{11}$$

For the continuous mechanical structure, the normal stress and normal displacement of interface are continuous

$$\left.\begin{array}{ll}\sigma_{z1} = \sigma_{z2} & (z=h) \\ w_1 = w_2 & (z=h)\end{array}\right\} \tag{12}$$

The shear stress of interface can be calculated by its displacement, as following

$$\tau_{zr1} = \tau_{zr2} = K(u_2 - u_1) \qquad (z=h) \tag{13}$$

Where K is the coefficient of layers combination.

In fact, when there is only vertical load, friction in layers has little effect on mechanical components distribution. we assume interface is smooth and frictionless to simplify the model. So $K=0$ and the shear stress of interface is as follows

$$\tau_{zr1} = \tau_{zr2} = 0 \qquad (z=h) \tag{14}$$

If r and z approach infinity($r \to \infty$ and $z \to \infty$), respectively, stress and displacement components in Eq. (9) will be zero

$$A_2 = C_2 = 0 \tag{15}$$

3.3 Solving the Stress and Displacement Components

By substituting stress/displacement of components in Eq. (9) into Eq. (11), (12), (14) and using Hankel integral transformation ,the following linear algebraic equations are obtained

$$\left.\begin{aligned}
&C_1 - (1-2\mu_1)A_1 - D_1 - (1-2\mu_1)B_1 = \bar{q}(\xi)\\
&C_1 + 2\mu_1 A_1 + D_1 - 2\mu_1 B_1 = 0\\
&\left[C_1 - (1-2\mu_1-\xi h)A_1\right]e^{\xi h} - \left[D_1 + (1-2\mu_1+\xi h)B_1\right]e^{-\xi h}\\
&= \left[C_2 - (1-2\mu_2-\xi h)A_2\right]e^{\xi h} - \left[D_2 + (1-2\mu_2+\xi h)B_2\right]e^{-\xi h}\\
&\left[C_1 + (2\mu_1+\xi h)A_1\right]e^{\xi h} + \left[D_1 - (2\mu_1-\xi h)B_1\right]e^{-\xi h} = 0\\
&\left[C_2 + (2\mu_2+\xi h)A_2\right]e^{\xi h} + \left[D_2 - (2\mu_2-\xi h)B_2\right]e^{-\xi h} = 0\\
&m\left[C_1 - (2-4\mu_1-\xi h)A_1\right]e^{\xi h} + \left[D_1 + (2-4\mu_1+\xi h)B_1\right]e^{-\xi h}\\
&= \left[C_2 - (2-4\mu_2-\xi h)A_2\right]e^{\xi h} + \left[D_2 + (2-4\mu_2+\xi h)B_2\right]e^{-\xi h}
\end{aligned}\right\} \tag{16}$$

Where

$$\begin{aligned}
&\bar{q}(\xi) = \int_0^\infty rq(r)J_0(\xi r)dr\\
&m = \frac{(1+\mu_1)E_2}{(1+\mu_2)E_1}
\end{aligned} \tag{17}$$

Substituting $A_2 = C_2 = 0$ into Eq. (16), A_i , B_i , C_i , D_i $(i = 1,2)$ could be represented as follows:

$$\left.\begin{aligned}
&A_1 = -\frac{\bar{q}(\xi)e^{-2\xi h}}{\Delta}[(N-1-\xi h) - (N-1)e^{-2\xi h}]\\
&B_1 = -\frac{\bar{q}(\xi)}{\Delta}[N - (N-\xi h)e^{-2\xi h}]\\
&C_1 = \frac{\bar{q}(\xi)e^{-2\xi h}}{\Delta}[(2\mu_1+\xi h)(N-1-\xi h) + N\xi h - 2\mu_1(N-1)e^{-2\xi h}]\\
&D_1 = -\frac{\bar{q}(\xi)}{\Delta}\{2\mu_1 N - [2N(\mu_1-\xi h) + (1-2\mu_1+\xi h)\xi h]e^{-2\xi h}\}\\
&B_2 = -\frac{\bar{q}(\xi)}{\Delta}(2N-1)[(1+\xi h) - (1-\xi h)e^{-2\xi h}]\\
&D_2 = -\frac{\bar{q}(\xi)}{\Delta}(2N-1)(2\mu_2-\xi h)[(1+\xi h) - (1-\xi h)e^{-2\xi h}]\\
&A_2 = C_2 = 0
\end{aligned}\right\} \tag{18}$$

Where

$$\Delta = N + [2\xi h(2N-1) - (1+2\xi^2 h^2)]e^{-2\xi h} - (N-1)e^{-4\xi h}] \tag{19}$$

$$N = \frac{(1-\mu_1)m}{2(1-\mu_2)} + \frac{1}{2} \tag{20}$$

Integral constant A_i , B_i , C_i , D_i is related to $\bar{q}(\xi)$. If the distribution equation of load $q(r)$ is known, components of stress and displacement is obtained by substituting $\bar{q}(\xi)$ into Eq. (18).

If the load is axial symmetrical and circular distribution of vertical loads, the distribution function of load circular range with assuming radius δ is expressed as:

$$q(r) = \begin{cases} q_\delta(r) & (0 \le r \le \delta) \\ 0 & (\delta < r < \infty) \end{cases} \tag{21}$$

Accordingly,

$$\bar{q}(\xi) = \int_0^\delta r q_\delta(r) J_0(\xi r) dr \tag{22}$$

In particular, if load circular is uniform $q_\delta(r) = q$,it is shown that

$$\bar{q}(\xi) = q\frac{\delta}{\xi} J_1(\xi\delta) \tag{23}$$

In order to separate $\bar{q}(\xi)$ from the integral constant expression, assuming $A_i = \tilde{A}_i\bar{q}(\xi)$, $B_i = \tilde{B}_i\bar{q}(\xi)$, $C_i = \tilde{C}_i\bar{q}(\xi)$, $D_i = \tilde{D}_i\bar{q}(\xi)$ in Eq. (18). If adding a new integral variable $x = \xi\delta$ and considering r , z into dimensionless form $\frac{r}{\delta}$, $\frac{z}{\delta}$, respectively. the final expression of the stress strain and displacement component is subjected to the vertical load is obtained by considering Eq. (23).

$$\left.\begin{aligned}
\sigma_{ri} &= q\int_0^\infty J_0\left(\frac{r}{\delta}x\right)J_1(x)\left\{\left[\tilde{C}_i + \left(1+2\mu_i + \frac{z}{\delta}x\right)\tilde{A}_i\right]e^{\frac{z}{\delta}x} - \left[\tilde{D}_i - \left(1+2\mu_i - \frac{z}{\delta}x\right)\tilde{B}_i\right]e^{-\frac{z}{\delta}x}\right\}dx - U_i \\
\sigma_{\theta i} &= 2\mu_i q\int_0^\infty J_0(\frac{r}{\delta}x)J_1(x)(\tilde{A}_i e^{\frac{z}{\delta}x} + \tilde{B}_i e^{-\frac{z}{\delta}x})dx + U_i \\
\sigma_{zi} &= -q\int_0^\infty J_0(\frac{r}{\delta}x)J_1(x)\left\{\left[\tilde{C}_i - \left(1-2\mu_i - \frac{z}{\delta}x\right)\tilde{A}_i\right]e^{\frac{z}{\delta}x} - \left[\tilde{D}_i + \left(1-2\mu_i + \frac{z}{\delta}x\right)\tilde{B}_i\right]e^{-\frac{z}{\delta}x}\right\}dx \\
\tau_{zri} &= -q\int_0^\infty J_1(\frac{r}{\delta}x)J_1(x)\left\{\left[\tilde{C}_i + \left(2\mu_i + \frac{z}{\delta}x\right)\tilde{A}_i\right]e^{\frac{z}{\delta}x} + \left[\tilde{D}_i - \left(2\mu_i - \frac{z}{\delta}x\right)\tilde{B}_i\right]e^{-\frac{z}{\delta}x}\right\}dx \\
u_i &= \frac{1+\mu_i}{E_i}q\delta\int_0^\infty \frac{J_1(\frac{r}{\delta}x)J_1(x)}{x}\left\{\left[\tilde{C}_i + \left(1+\frac{z}{\delta}x\right)\tilde{A}_i\right]e^{\frac{z}{\delta}x} - \left[\tilde{D}_i - \left(1-\frac{z}{\delta}x\right)\tilde{B}_i\right]e^{-\frac{z}{\delta}x}\right\}dx \\
w_i &= -\frac{1+\mu_i}{E_i}q\delta\int_0^\infty \frac{J_0(\frac{r}{\delta}x)J_1(x)}{x}\left\{\left[\tilde{C}_i - \left(2-4\mu_i - \frac{z}{\delta}x\right)\tilde{A}_i\right]e^{\frac{z}{\delta}x} + \left[\tilde{D}_i + \left(2-4\mu_i + \frac{z}{\delta}x\right)\tilde{B}_i\right]e^{-\frac{z}{\delta}x}\right\}dx
\end{aligned}\right\} \tag{24}$$

Where

$$U_i = q\int_0^{\infty} \frac{J_1(\frac{r}{\delta}x)J_1(x)}{\frac{r}{\delta}x}\left\{\left[\tilde{C}_i + \left(1+\frac{z}{\delta}x\right)\tilde{A}_i\right]e^{\frac{z}{\delta}x} - \left[\tilde{D}_i - \left(1-\frac{z}{\delta}x\right)\tilde{B}_i\right]e^{-\frac{z}{\delta}x}\right\}dx$$

$$\begin{aligned}
&\tilde{A}_1 = -\frac{e^{-2\frac{h}{\delta}x}}{\Delta}[(N-1-\frac{h}{\delta}x)-(N-1)e^{-2\frac{h}{\delta}x}] \\
&\tilde{B}_1 = -\frac{1}{\Delta}[N-(N-\frac{h}{\delta}x)e^{-2\frac{h}{\delta}x}] \\
&\tilde{C}_1 = \frac{e^{-2\frac{h}{\delta}x}}{\Delta}[(2\mu_1+\frac{h}{\delta}x)(N-1-\frac{h}{\delta}x)+N\frac{h}{\delta}x-2\mu_1(N-1)e^{-2\frac{h}{\delta}x}] \\
&\tilde{D}_1 = -\frac{1}{\Delta}\{2\mu_1 N-[2N(\mu_1-\frac{h}{\delta}x)+(1-2\mu_1+\frac{h}{\delta}x)\frac{h_1}{\delta}x]e^{-2\frac{h}{\delta}x}\} \\
&\tilde{B}_2 = -\frac{1}{\Delta}(2N-1)[(1+\frac{h}{\delta}x)-(1-\frac{h}{\delta}x)e^{-2\frac{h}{\delta}x}] \\
&\tilde{D}_2 = -\frac{1}{\Delta}(2N-1)(2\mu_2-\frac{h}{\delta}x)[(1+\frac{h}{\delta}x)-(1-\frac{h}{\delta}x)e^{-2\frac{h}{\delta}x}] \\
&\tilde{A}_2 = \tilde{C}_2 = 0
\end{aligned} \tag{25}$$

$$\Delta = N+[2\frac{h}{\delta}x(2N-1)-(1+2\frac{h^2}{\delta^2}x^2)]e^{-2\frac{h}{\delta}x}-(N-1)e^{-4\frac{h}{\delta}x}] \tag{26}$$

3.4 *Calculation Example*

Assuming first layer's parameters $h=9mm$, $\delta=15mm$, Specimen's material $Q235$, Young's modulus $E_1=E_2=2\times10^5 MPa$,Poisson's ratio $\mu_1=\mu_2=0.3$. The vertical load on the surface is $Q=9000N$, $q=Q/\pi\delta^2$. The stress and displacement field are calculated by Eq. (24), as shown in Fig. 5.

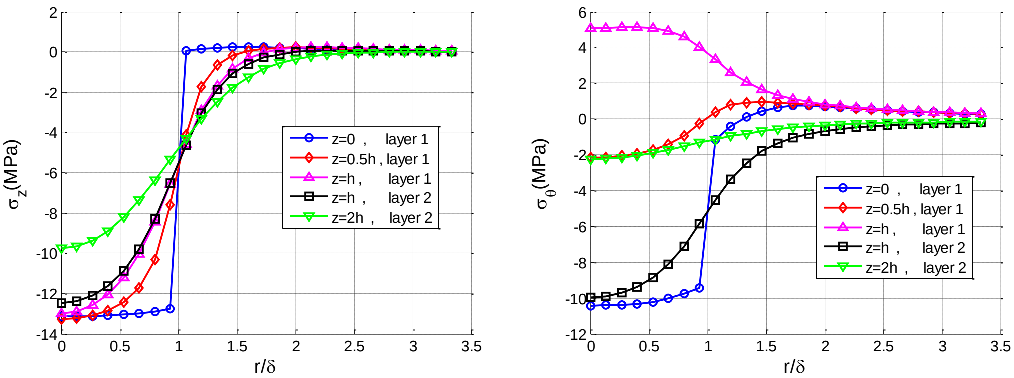

(a) (b)

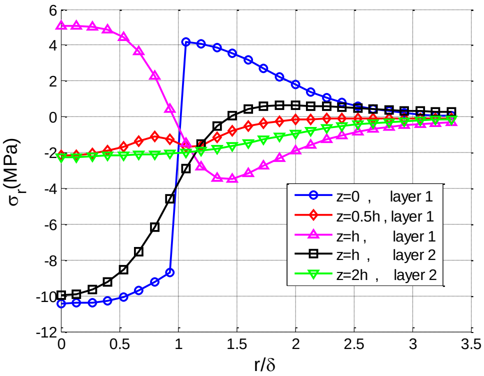

(c)

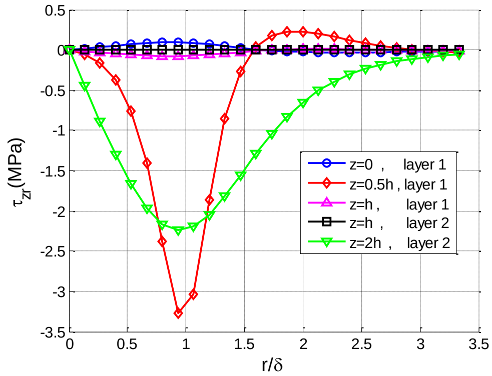

(d)

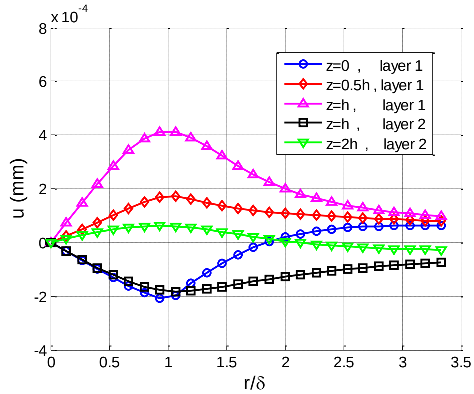

(e)

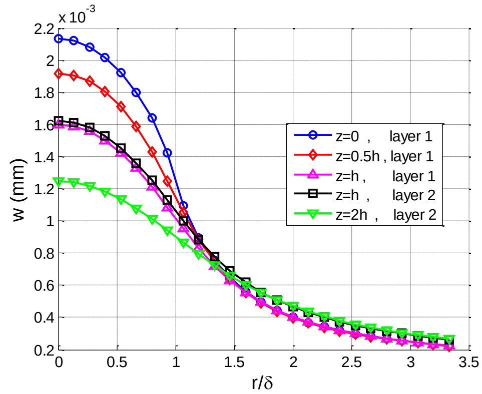

(f)

Fig. 4. Stress and displacement distribution curves along radial direction

In Fig. 4(a), the curve $z=0$ mutates at r=δ and when r>δ, $\sigma_z=0$; when r<δ, $\sigma_z=-q$, satisfying surface stress boundary condition. The curve $z=h,\ layer\ 1$ and curve $z=h_1,\ layer\ 2$ are over-lapped, corresponding with interlayer stress boundary condition $\sigma_{z1}=\sigma_{z2}$. In Fig. 4(f), curve $z=h,\ layer\ 1$ and curve $z=h,\ layer\ 2$ are overlapped, satisfying interlayer displacement boundary condition $w_1=w_2$. In Fig. 4 (d), the value of curve $z=0,\ layer\ 1$ and curve $z=h,\ layer\ 1$ are close to 0, satisfying shear stress equals to 0 in surface and interlayer. When r gradually increasing, all the components in Fig. 4 will tend to zero, corresponding to the condition when r approaches infinite, all of components will be zero. These results prove the reasonability of LET.

4 Experiment and finite element analysis

In order to verify the LET's effectiveness in the calculation of stress /displacement field of structural discontinuity, we extract the normal stress on interface and compare it with the results of experimental and finite element analysis.

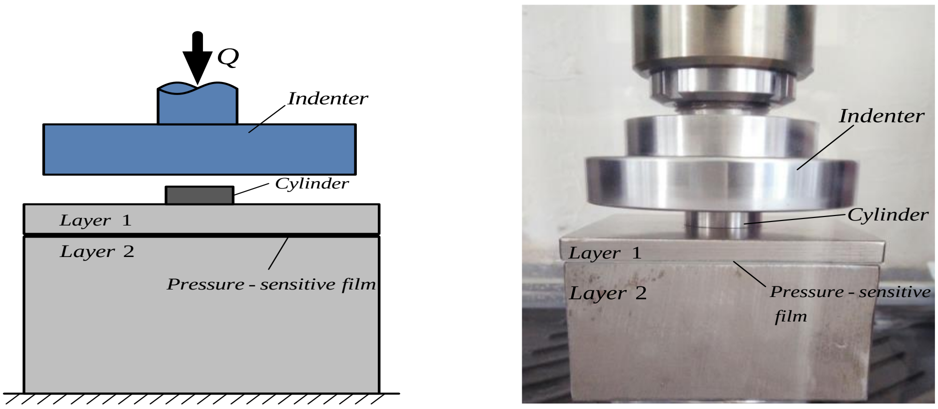

(a) (b)

Fig. 5. Experimental schematic diagram and field photos.

Taking two cuboid metals as experimental specimen and both the material of them are $Q235$,Young's modulus $E_1 = E_2 = 2\times10^5 MPa$, Poisson's ratio $\mu_1 = \mu_2 = 0.3$. We denote the size of metal block as $100mm\times100mm\times9mm$ in the first layer and the size of another metal block as $100mm\times100mm\times60mm$. The contact region between two metals were grounded to $R_a = 0.8\mu m$. The contact stress was measured by the pressure-sensitive film, which is placed on the interface. The cupping machine was used to provide load and the load was transformed into circular load by a metal cylinder of radius $\delta = 15mm$, high $10mm$, placed on the top of the first layer. At first, the cupping machine loaded downwards slowly until the pressure reaches $9000N$. Then the pressure was kept for some time so that the color of pressure-sensitive film was fully displayed. Photos of experimental schematics and site are shown in Fig. 5.

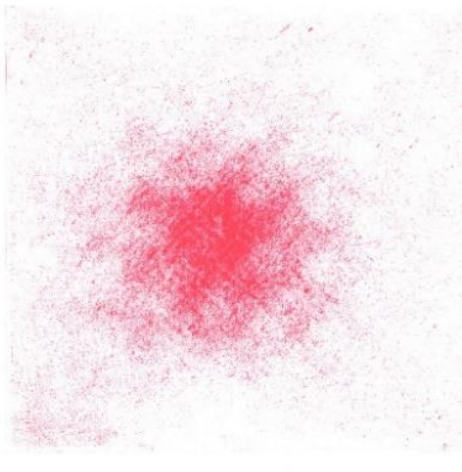

Fig. 6. Pressure-sensitive film

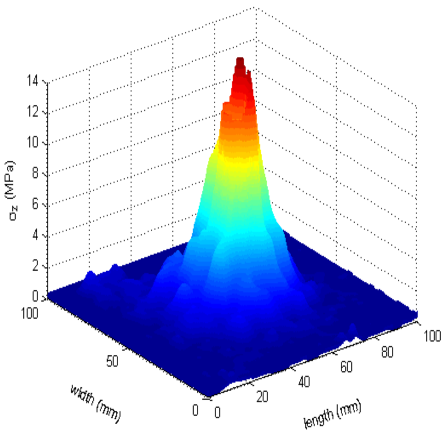

Fig.7. Pressure distribution of interface.

Because of the pressure, the white pressure-sensitive film turns red, and the red concentration increases with the increase of pressure intensity. The contact stress can be measured by evaluating the color concentration of the film. Fig. 6 shows the scanning image of the pressure-sensitive film after experiment. Obviously, the color distributed as an axisymmetric pattern. The high color concentration in the center indicates that the contact pressures are large. The color concentration rapidly decreases in the region far from center, indicating that the pressure drops quickly. After denoising and fliting, the color density of film was converted into pressure value and a three-dimensional image which displaying pressure distribution of interface in Fig. 6 and Fig. 7. The "steep peak" distribution of the contact pressure is shown clearly in the figure.

Due to machining error and measurement error, the result in Fig. 6 is not absolutely axisymmetric. In order to eliminate the impact of these errors, we used the average value of axial pressure to represent the pressure in the radial.

Fig. 8 shows the contact stress distribution of LET, experimental and finite element method (FEM). Because the existing of pressure-sensitive film, the state of contact pressure on interface has been changed in a way. There were two comparative analysis of FEM with different contact conditions. FEM (with film) adds a new layer which has same mechanical parameter with film between the original layers and FEM (without film) contacts directly. The value of pressure in the figure is negative, indicating the compressive stress.

In Fig. 8, four pressure distribution curves basically coincide. The curve of LET and FEM (without film) almost overlapped since both of them regardless the influence of film layer. The curve of experimental and FEM (with film) is lower in center and higher in edges than LET and FEM (without film). It indicates that the presence of films has a certain effect on the state of mechanical interface. In general, the pressure distribution of experimental and finite element analysis is consistent with the result of layered elastic system.

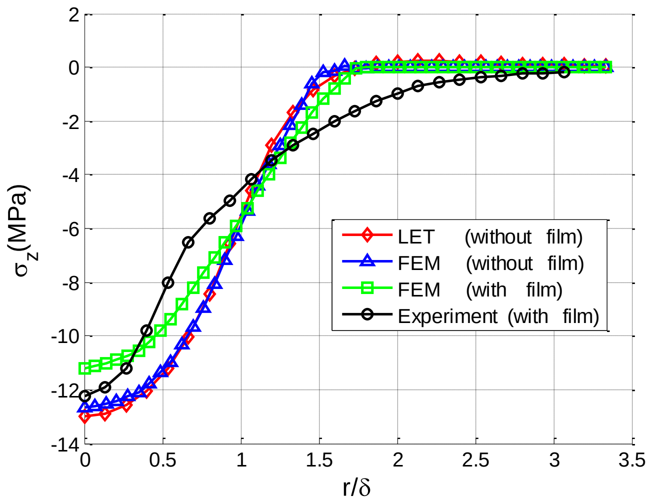

Fig. 8. Data comparison of contact stress

5 Conclusions

A stress/displacement field calculation model based on layered elastic mechanics is established to solve the mechanical calculation problem in the discontinuous structure in joints.

The calculation model based on layered elastic mechanics is a new way to calculate the stress / displacement field in joints. This method can be extended to more mechanical structure, considering different types of load, friction and other complex conditions and it is effective to analyze problems such as pressure distribution and small sliding of interface.

The model still has some shortcomings: For instance, because of ignoring the and roughness, flatness and waviness of the contact surfaces, there will be a deviation between the calculation results and the actual situation to some extent. The analytical model of the mechanics characteristics of the complex geometry parts subjected to non-axisymmetric loads or horizontal load (unidirectional load, rotational load) needs further study.

References

[1] Ibrahim R A, Pettit C L. Uncertainties and dynamic problems of bolted joints and other fasteners. Journal of sound and Vibration, 279(3), 857-936.

[2] Chen, W., & Deng, X. Structural damping caused by micro-slip along frictional interfaces. International Journal of Mechanical Sciences 47(8), 1191-1211 (2016).

[3] Bosman, R., Hol, J., & Schipper, D. J. Running-in of metallic surfaces in the boundary lubrication regime. Wear, 271(7), 1134-1146 (2011).

[4] Burdekin, M., Back, N., & Cowley, A. Analysis of the local deformations in machine joints. ARCHIVE Journal of Mechanical Engineering Science 1959-1982 (vols 1-23), 21(1), 25-32 (1979).

[5] Yigit, A. S., & Ulsoy, A. G. Dynamic stiffness evaluation for reconfigurable machine tools including weakly non-linear joint characteristics. Proceedings of the Institution of Mechanical Engineers Part B Journal of Engineering Manufacture, 216(1), 87-101 (2002).

[6] Back N, Burdekin M, Cowley A. Review of the research on fixed and sliding joints. In 13th International Machine Tool Design and Research Conference, 87-97. MacMillan, London, (1973).

[7] Beards C F. The damping of structural vibration by controlled interfacial slip in joints. Journal of Vibration and Acoustics, 105(3), 369-373 (1983).

[8] Beards C F, Woowat A. The control of frame vibration by friction damping in joints. Journal of Vibration and Acoustics, 107(1), 26-32 (1985).

[9] Beards C F. Damping in structural joints. Vibration Inst., The Shock and Vibration Digest, 21(4), 3-5 (1989).

[10] Fu W P, Huang Y M, Zhang X L. Experimental investigation of dynamic normal characteristics of machined joint surfaces. ASME Journal of Vibration and Acoustics, 122(4), 393 (2000).

[11] Zhang X L, Wen S H, Lan G S, et al. Experiment research on tangential dynamic characteristics of machined plane joint interfaces. In Advanced Materials Research., 145: 584-589 (2011).

[12] Mi L, Yin G, Sun M, et al. Effects of preloads on joints on dynamic stiffness of a whole machine tool structure. Journal of mechanical science and technology, 26(2), 495-508 (2012).

[13] Shimizu S, Kabaya Y, Sakamoto H, et al. Identification Method of Dynamic Characteristics of Joints in Jointed Structures. Journal ref: International Journal of Automation Technology, 7(2), 221-227 (2013).

[14] Guo T, Li L, Cai L, et al. Alternative method for identification of the dynamic properties of bolted joints. Journal of mechanical science and technology, 26(10), 3017-3027 (2012).

[15] Tian H, Li B, Liu H, et al. A new method of virtual material hypothesis-based dynamic modeling on fixed joint interface in machine tools. International Journal of Machine Tools and Manufacture, 51(3), 239-249 (2011).

[16] Mase G T, Smelser R E, Mase G E. Continuum mechanics for engineers. CRC press, (2011).

[17] Burmister D M. The general theory of stresses and displacements in layered systems. I. Journal of applied physics, 16, 89-94 (1945).

[18] Burmister D M. The general theory of stresses and displacements in layered soil systems. II. Journal of applied Physics, 16, 126-127 (1945).

[19] Burmister D M. The general theory of stresses and displacements in layered soil systems. III. Journal of applied Physics, 16, 296-302 (1945).

[20] Muki R. A three-dimensional problem of a semi-infinite elastic solid under the compressive action of a rigid body. Proceedings of the Fujihara Memorial Faculty of Engineering Keio University, 8(30), 68 (8)-80 (20) (1955).

[21] Kai W. Analysis and calculation of stresses and displacements in layered elastic systems. Acta Mechanica Sinica, 3(3), 251-260 (1987).

[22] Maina J W, Matsui K. Developing software for elastic analysis of pavement structure responses to vertical and horizontal surface loadings. Transportation Research Record Journal of the Transportation Research Board, 1896(1), 107-118 (2004).

[23] Wang D, Roesler J R, Guo D Z. Innovative algorithm to solve axisymmetric displacement and stress fields in multilayered pavement systems. Journal of Transportation Engineering, 137(4), 287-295 (2010).